coatings

MDPI

Article

Effect of Fluorinated Comonomer, Polymerizable Emulsifier, and Crosslinking on Water Resistance of Latex Coatings

Jana Machotova [1,*], Petr Knotek [2], Eva Cernoskova [3], Roman Svoboda [4], Lucie Zarybnicka [5,6], Miroslav Kohl [1] and Andrea Kalendova [1]

1 Institute of Chemistry and Technology of Macromolecular Materials, Faculty of Chemical Technology, University of Pardubice, Studentská 573, 532 10 Pardubice, Czech Republic
2 Department of General and Inorganic Chemistry, Faculty of Chemical Technology, University of Pardubice, Studentská 573, 532 10 Pardubice, Czech Republic
3 Joint Laboratory of Solid State Chemistry, Faculty of Chemical Technology, University of Pardubice, Studentská 84, 532 10 Pardubice, Czech Republic
4 Department of Physical Chemistry, Faculty of Chemical Technology, University of Pardubice, Studentská 84, 532 10 Pardubice, Czech Republic
5 Department of Technical Studies, College of Polytechnics Jihlava, Tolstého 16, 586 01 Jihlava, Czech Republic
6 Institute of Theoretical and Applied Mechanics of the Czech Academy of Sciences, Centre Telč, Prosecká 809/76, 190 00 Praha, Czech Republic
* Correspondence: jana.machotova@upce.cz; Tel.: +420-466-037-194

Abstract: Common latex coatings suffer from poor water resistance, which often limits their practical application. This paper reports on the preparation of polyacrylate latexes using various approaches to tune the water resistance, wettability, and surface properties of their coating films. The mutual effects of fluorinated monomer copolymerization, emulsifier type (polymerizable and general), and intra- or interparticle covalent crosslinking (due to allyl methacrylate copolymerization and a keto-hydrazide reaction, respectively) were studied. The polyacrylate latexes were synthesized through a two-step semicontinuous emulsion polymerization of 2,2,2-trifluoroethyl methacrylate, butyl acrylate, methyl methacrylate, and methacrylic acid as the basic monomers. The fluorinated monomer was incorporated into the second-step polymer (at a content of 30 wt.% based on the second-step monomer feeds). The water resistance, wettability, and surface properties of the coating films were evaluated with focus on the water absorption, water whitening, water contact angle, and surface topography using atomic force microscopy. It was found that highly water-resistant and hydrophobic coatings that possessed a self-healing ability were prepared, provided that the polymerizable emulsifier and the fluorinated monomer were involved in the latex synthesis, along with the intra- and interparticle covalent crosslinking.

Keywords: polyacrylate latex; polymerizable emulsifier; crosslinking; keto-hydrazide reaction; water resistance; hydrophobicity; self-healing

Citation: Machotova, J.; Knotek, P.; Cernoskova, E.; Svoboda, R.; Zarybnicka, L.; Kohl, M.; Kalendova, A. Effect of Fluorinated Comonomer, Polymerizable Emulsifier, and Crosslinking on Water Resistance of Latex Coatings. *Coatings* **2022**, *12*, 1150. https://doi.org/10.3390/coatings12081150

Academic Editor: Florina Branzoi

Received: 29 June 2022
Accepted: 5 August 2022
Published: 9 August 2022

1. Introduction

Emulsion polymerization represents a feasible and eco-friendly method for the preparation of waterborne latex coatings with favorable properties, such as good film-forming properties, low cost, facile synthesis, easy pigmentation, and treatment. However, common latex coatings suffer from moisture and water sensitivity, which limits their practical use in the field of high-performance material protection. One way to improve the water resistance of a coating film is the creation of a hydrophobic coating surface. Hydrophobicity is commonly characterized by the water contact angle (WCA), which exceeds 90° for hydrophobic surfaces. Nevertheless, the WCA of most common latex films rarely reaches the hydrophobic threshold. For example, in the case of acrylic or styrene-acrylic latex coatings comprising standard surfactants, WCAs not exceeding 80° have been reported in the relevant literature [1–3].

Hydrophobic or water-repellent coatings are highly demanded due to many useful properties such as antifouling [4,5], anticorrosion [6–8], low dirt pickup, and self-cleanability [9–11]. Copolymerization with a fluorinated acrylic monomer has traditionally been used to introduce hydrophobicity into latex coatings [12–15]. Fluorinated groups, which can impart several extraordinary properties to coatings [16,17], tend to enrich the film-air interface during latex film formation to reduce interfacial energy. This behavior may result in coatings with decreased wettability [18–21]. On the other hand, these groups can hide inside the coating if immersed in water [22,23]. This behavior may cause a loss in the hydrophobicity of fluorinated latex coatings [24]. A traditionally used tool to overcome the drawback mentioned above is the fixation of fluorinated groups on the polymer particle surface by employing intraparticle or interparticle crosslinking chemistry [25–28]. Intraparticle crosslinking can be formed during latex synthesis by incorporating multifunctional monomers, such as allyl methacrylate (ALMA) [2], while interparticle crosslinking can be generated by a chemical reaction between neighboring polymer particles under appropriate cure conditions in the course of film formation [19,29,30]. Nowadays, one-pack, self-crosslinking coating systems curable at ambient temperature are demanded [31–33]. Among these materials, latex formulations using the keto-hydrazide crosslinking reaction are particularly favored [34–36]. Copolymerized diacetone-acrylamide (DAAM) cured with adipic acid dihydrazide (ADH) dissolved in an aqueous latex medium is a popular combination of self-crosslinking latex coating compositions [37–39].

The application of polymerizable emulsifiers in the emulsion polymerization process appears to be another possible approach to improving the water and moisture resistance of latex coating films [14,40–43]. When conventional (nonpolymerizable) emulsifiers are part of latex coatings, their molecules can desorb from the surface of polymer particles, migrate through the coating film, and form aggregates in the interstitial areas, resulting in increased water penetration [44]. Nonpolymerizable emulsifier molecules can also migrate at the film-air interface, resulting in a decrease in coating hydrophobicity and gloss, or at the film-substrate interface, which can lead to a loss of adhesion [45]. When polymerizable emulsifiers that bond covalently to polymer particles are utilized in latex synthesis, the risk of their desorption and migration through the latex film is eliminated [46,47]. The resulting coating films then generally exhibit higher water resistance and hydrophobicity [48–52].

In the search for an optimal and highly effective latex composition for applications such as hydrophobic and water-resistant coatings suitable for the universal protection of various substrates used both indoors and outdoors, we focused on the interaction of different approaches, namely (I) the copolymerization of a fluorinated monomer, (II) the application of a polymerizable emulsifier, (III) the use of interparticle covalent crosslinking due to a keto-hydrazide reaction, and (IV) the implementation of intraparticle covalent crosslinking by ALMA copolymerization. Water resistance, hydrophobicity, and surface properties were the main criteria that were evaluated and compared.

2. Materials and Methods

2.1. Materials

2,2,2-Trifluoroethyl methacrylate (TFEMA, CAS: 352-87-4), butyl acrylate (BA, CAS: 141-32-2), methyl methacrylate (MMA, CAS: 80-62-6), methacrylic acid (MAA, CAS: 79-41-4), diacetone acrylamide (DAAM, CAS: 2873-97-4), and allyl methacrylate (ALMA, CAS: 96-05-9) were used as starting monomers (Sigma-Aldrich, Prague, Czech Republic). Disponil FES 993 (BASF, Prague, Czech Republic) was employed as a general (nonpolymerizable) emulsifier. HITENOL AR-10 (DKS Co., Ltd., Tokyo, Japan) was utilized as a polymerizable emulsifier. Table 1 shows the characteristic properties of both kinds of emulsifiers. Ammonium persulfate (Penta, Prague, Czech Republic, CAS: 7727-54-0) was used as the free-radical initiator. Adipic acid dihydrazide (ADH, TCI Europe, Zwijndrecht, Belgium, CAS: 1071-93-8) served as the covalent curing agent. All chemicals were used as delivered.

Table 1. Characteristics of the emulsifiers.

Emulsifier	Type	Chemical Composition	Active Matter (wt.%)	Critical Micelle Concentration (mg/L) [a]
Disponil FES 993	General	Sodium salt of fatty alcohol polyglycol ether sulfate	29.7	200
HITENOL AR-10	Polymerizable	Ammonium salt of polyoxyethylene styrenated propenyl phenyl ether sulfate	99.1	250

[a] Data provided by the manufacturer.

2.2. Synthesis and Testing of Latexes

Four series of polyacrylate latexes differing in fluorination of the second-step polymer, covalent crosslinking strategy, and emulsifier type were synthesized through a technique of nonseeded semibatch emulsion polymerization. This process is unique in its high, immediate conversion of monomers exceeding 90%. Therefore, so-called monomer-starved conditions were maintained during free-radical polymerization and a relatively homogeneous chemical composition of statistical copolymers could be achieved [53]. Monomeric compositions of the prepared copolymers are given in Table 2, and the recipe for the synthesis of the latexes is shown in Table 3. A two-step procedure was followed, which is a common approach for the synthesis of fluorinated latex compositions. In this way, fluorinated monomers (or monomers functionalized with reactive groups) are introduced in the second step, providing a predominant location of fluorinated (or reactive) groups in the outer layer of the polymer particles [22,54–59]. The weight ratio of the first-step to second-step copolymers was 1:1, which corresponds to the thickness of the second-step copolymer layer of approximately 20% of the radius of the polymer particle if full phase separation is considered.

The Fox equation [60] was used to determine the adequate ratios of acrylic monomers, resulting in a latex copolymer having a T_g of approximately 5 °C (at this temperature, sufficient film formation is supposed to be maintained even in highly crosslinked films). Each series included four latex samples: two samples were always prepared with a general (nonpolymerizable) emulsifier (sample design D), and two samples were synthesized using a polymerizable emulsifier (sample design H). The amounts of the emulsifiers were set to maintain the same content of surface-active matter in both types of latex samples. In every series, one of the D-designed samples and one of the H-designed samples (designs D_F and H_F) comprised of copolymerized TFEMA was incorporated during the polymerization process of the second-step copolymer. The content of copolymerized TFEMA in the second-step copolymer was 30 wt.%.

In Series 1, covalent crosslinking was not implemented. In Series 2, a covalent interparticle crosslinking strategy using the keto-hydrazide reaction was employed. For this reason, DAAM (5 wt.% in the second-step monomer feeds) was incorporated into the second-step copolymer. In Series 3, covalent intraparticle crosslinking was implemented by incorporating ALMA (1 wt.% based on the first-step monomer feeds) in the first-step copolymer. Series 4 was represented by latexes using covalent inter- and intraparticle crosslinking achieved by DAAM and ALMA copolymerization, performed in the same manner as described above.

Latexes were prepared in a stirred flask under inert gas (N_2) at 85 °C. Water, the respective emulsifier, and initiator were inserted into a reaction flask (see Table 3), and the reaction flask charge was warmed to 85 °C. The first-step monomer emulsion was then dosed dropwise into the flask over 60 min, followed by 15 min polymerization of the first-step copolymer. Subsequently, the second-step monomer emulsion was dosed dropwise into the flask over 60 min. The reaction mixture was then allowed to polymerize for an additional 2 h. The pH of the latex samples was adjusted to 8.5 with ammonia. In the end, aqueous ADH solution (1.25 g dissolved in 11.3 g of water) was mixed in the latexes of Series 2 and 4. In this way, final latexes having a solids content of approximately 39 wt.%

were prepared. The average diameters of the polymer particles were determined by means of dynamic light scattering (DLS) with a Litesizer 500 (Anton Paar, Graz, Austria).

Table 2. Compositions of latexes differing in the fluorinated monomer copolymerization into the second-step polymer, emulsifier type, and covalent crosslinking strategy.

Sample	Composition of Monomer Feeds (g) TFEMA/MMA/BA/MAA/DAAM/ALMA		Emulsifier Type	Fluorination of the Second-Step Copolymer
	First Step	Second Step		
Series 1: No crosslinking				
D_1	0/18.5/30/1.5/0/0	0/18.5/30/1.5/0/0	general	no
H_1	0/18.5/30/1.5/0/0	0/18.5/30/1.5/0/0	polymerizable	no
D_{1_F}	0/18.5/30/1.5/0/0	15/6.5/27/1.5/0/0	general	yes
H_{1_F}	0/18.5/30/1.5/0/0	15/6.5/27/1.5/0/0	polymerizable	yes
Series 2: Keto-hydrazide crosslinking				
D_2	0/18.5/30/1.5/0/0	0/16.5/29.5/1.5/2.5/0	general	no
H_2	0/18.5/30/1.5/0/0	0/16.5/29.5/1.5/2.5/0	polymerizable	no
D_{2_F}	0/18.5/30/1.5/0/0	15/4.5/26.5/1.5/2.5/0	general	yes
H_{2_F}	0/18.5/30/1.5/0/0	15/4.5/26.5/1.5/2.5/0	polymerizable	yes
Series 3: ALMA crosslinking				
D_3	0/18/30/1.5/0/0.5	0/18.5/30/1.5/0/0	general	no
H_3	0/18/30/1.5/0/0.5	0/18.5/30/1.5/0/0	polymerizable	no
D_{3_F}	0/18/30/1.5/0/0.5	15/6.5/27/1.5/0/0	general	yes
H_{3_F}	0/18/30/1.5/0/0.5	15/6.5/27/1.5/0/0	polymerizable	yes
Series 4: Keto-hydrazide and ALMA crosslinking				
D_4	0/18/30/1.5/0/0.5	0/16.5/29.5/1.5/2.5/0	general	no
H_4	0/18/30/1.5/0/0.5	0/16.5/29.5/1.5/2.5/0	polymerizable	no
D_{4_F}	0/18/30/1.5/0/0.5	15/4.5/26.5/1.5/2.5/0	general	yes
H_{4_F}	0/18/30/1.5/0/0.5	15/4.5/26.5/1.5/2.5/0	polymerizable	yes

Table 3. Components of the polymerization mixture with different emulsifiers.

Component	Reaction Flask (g)	First-Step Monomer Emulsion (g)	Second-Step Monomer Emulsion (g)
Distilled water	33.00	50.00	72.00
Disponil FES 993 [a]	0.24	3.70	3.70
HITENOL AR-10 [b]	0.07	1.10	1.10
Ammonium persulfate	0.20	0.20	0.20
Monomers	0.00	50.00	50.00

[a] General (nonpolymerizable) emulsifier used in the syntheses of the D-designed latexes. [b] Polymerizable emulsifier used in the syntheses of the H-designed latexes.

2.3. Preparation and Testing of Free-Standing Coating Films

Latexes were poured into silicone molds. The free-standing coating films were allowed to dry at room temperature (RT, 23 ± 1 °C) for at least 4 weeks. The free-standing films, having a thickness of about 0.7 mm, were used for the investigation of water absorption, chemical structure, and the degree of crosslinking.

The water absorption was determined from swelling experiments on film samples (2×2 cm^2) immersed in distilled water for 30 days at RT. At the end of the swelling experiment, the soaked films were removed, carefully wiped using wood pulp, and weighed. The water absorption (A) was calculated using Equation (1) [61,62]:

$$A = 100 \frac{w_t - w_0}{w_0} \quad (1)$$

where w_0 is the initial weight of the sample (before immersion in water), and w_t is the weight of the swollen sample.

The chemical compositions of the latex films were analyzed using Fourier-transform infrared (FT-IR) spectroscopy with a Nicolet iN10 instrument (Thermo Fisher Scientific, Waltham, MA, USA). IR spectra were obtained using the attenuated total reflectance (ATR) with a diamond crystal in the range of 3500 cm^{-1} to 600 cm^{-1}. The degree of crosslinking of the latex films was evaluated from the point of view of crosslink density, as well as the average molar mass between crosslink junctions (M_c). The M_c and the crosslink density were detected using swelling of the dry gel polymer samples (approximately 0.3 g) in toluene. Swelling took place for 10 days at 50 °C. At the end of the swelling period, the samples were withdrawn from the toluene, rapidly dried with a filter paper, and weighed. The M_c and the crosslink density (moles of crosslinks/cm^3 of the polymer network) were calculated using Equations (2)–(5) [63,64]:

$$M_c = \frac{V_1 \rho_p \left[\phi^{1/3} - \phi/2\right]}{-[ln(1-\phi) + \phi + \chi\phi^2]} \quad (2)$$

$$\phi = \frac{W_p \rho_s}{W_p \rho_s + W_s \rho_p} \quad (3)$$

$$\chi = 0.34 + \frac{V_1}{RT}(\delta_1 - \delta_2)^2 \quad (4)$$

$$\text{Crosslink density} = \frac{\rho_p}{M_c} \quad (5)$$

where V_1 is the molar volume of toluene (106.3 cm^3/mol); ρ_p is the copolymer density calculated to be 1.103 g/cm^3 for the MMA/BA/MAA copolymer (37/60/3 by weight) from 1.18, 1.06, and 1.015 g/cm^3 for poly(MMA), poly(BA), and poly(MAA), respectively; ϕ is the volume fraction of the gel copolymer in the swollen gel; W_s and W_p are the weight fractions of toluene and the gel copolymer in the swollen gel, respectively; ρ_s is the density of toluene (0.8669 g/cm^3); χ is the copolymer and solvent interaction parameter; δ_1 is the copolymer solubility parameter that was calculated to be 9.135 $(cal/cm^3)^{1/2}$ for the MMA/BA/MAA copolymer (37/60/3 by weight) from 9.3, 9.0, and 9.8 $(cal/cm^3)^{1/2}$ for poly(MMA), poly(BA), and poly(MAA), respectively [65,66]; and δ_2 is the solubility parameter of toluene at 8.9 $(cal/cm^3)^{1/2}$.

2.4. Preparation and Testing of Coatings

Coatings were draw-downed onto glass substrates using a blade applicator with a slot width of 120 µm. The coatings were allowed to dry at RT and a relative humidity (RH) of 45 ± 1% for 7 days using a CTC Memmert climatic chamber (Memmert GmbH + Co.KG, Schwabach, Germany). Water whitening, WCA, macrosurface appearance, surface topography, and self-healing performances were evaluated.

The water whitening of coatings exposed to distilled water for 24 h at RT was evaluated according to the decrease in transmittance at a wavelength of 500 nm. A ColorQuest XE Spectrometer (Hunterlab, Reston, VA, USA) was used for the transmittance measurements. The level of water whitening (W) was calculated using Equation (6):

$$W = 100\,\frac{T_0 - T_t}{T_0} \quad (6)$$

where T_0 is the transmittance of the coating before water exposure, and T_t is the transmittance of the coating measured immediately after the water exposure.

WCA measurements were performed by the sessile drop method by means of an Attension Theta optical tensiometer (Biolion Scientific, Espoo, Finland). A water drop volume of 1 µL was used, and the steady-state WCA value was taken at the time of 10 s. Ten measurements were performed for each latex coating at RT and 45 ± 5% RH. To

investigate the effect of water exposure on the wettability of coatings, the WCAs of the coatings after their 1-day immersion in distilled water were also examined. The testing procedure was as follows: a dried coating (drying took place under the conditions specified above) was dipped in water for 24 h at RT. After that, the coating was allowed to dry out again in a climatic chamber at RT and 45 ± 1% RH for 7 days. Then, the WCA measurements were performed.

The macrosurface appearance of the latex films was observed using a Keyence VHX-6000 digital optical microscope (Keyence, Itasca, IL, USA) with a VHX-S600E free-angle observation system (Z-motorized). The macrosurface topography was analyzed on a 4 × 4 mm^2 sample area.

The topography of the latex film surface was monitored utilizing atomic force microscopy (AFM). AFM was carried out using a Dimension Icon (Bruker, Billerica, MA, USA) in PeakForce Quantitative Nanoscale Mechanical mode employing ScanAsyst-Air tips (k = 0.4 N m^{-1}). The images were recorded at a scan frequency of 0.5 Hz in a resolution of 512 × 512 pixels. For further details, see the references [67,68]. The self-healing (recovery) effect was studied by the scratch method [69] at RT and 30 ± 1% RH. The residual topography was analyzed with a DHMR 1000 digital holographic microscope (Lynceé Tec, Lausanne, Switzerland) operating at 785 nm in the reflection configuration using microscopic objectives with 10× and 20× magnifications [70].

3. Results and Discussion

3.1. Characterization of Liquid Latexes and Dried Copolymers

All the synthesized latexes, regardless of the emulsifier type and copolymer composition, contained a negligible amount of coagulum (0–0.2 wt.%), which indicated good colloidal stability during the polymerization. The average particle sizes and polydispersity indices of the latex samples were tracked after the completion of the first polymerization step and after completing the polymerization (see Table 4). The comparison of the average particle diameters between the first-step polymer particles and the respective resulting latex samples revealed that the diameters of the final latex particles increased in line with the presumed growth of the particle size (being approximately 20% of the particle diameter in the case of performing two-step emulsion polymerization of monomers in a weight ratio of 1:1, as mentioned above). This fact, together with low polydispersity indices, indicates that no significant secondary nucleation of new particles occurred during the second polymerization step in the case of all the polymerizations. In addition, it also allows us to suggest that TFEMA and DAAM structural units were located predominantly in the outer layers of polymer particles, reflecting the order of monomer dosing. When comparing the particle diameters for latex particles of the same copolymer composition but differing in the emulsifier type, lower diameters of the final particles were detected in the case of the polymerizable emulsifier-based latexes. This finding suggests an increased number of latex particles formed during polymerization using the polymerizable emulsifier, leading to smaller dimensions of the polymer particles [71–73].

The effects of the covalent crosslinking, type of emulsifier, and fluorination of the second-step polymer on the chemical composition of the prepared copolymers were studied by means of FT-IR spectroscopy. The absorption spectra of the copolymers of Series 1 (without crosslinking) and Series 2 (with interparticle covalent crosslinking) are depicted in Figures 1 and 2. It was evident that no pronounced distinctions between the chemical compositions of corresponding copolymers differing in emulsifier type could be observed. All the spectra exhibited a weak absorption band at 620 cm^{-1}, which is characteristic of sulfate groups (SO_4^{2-}) and indicates the employment of both types of emulsifiers. The spectra of all the polymers further showed absorption bands at 2963 and 2866 cm^{-1} corresponding to asymmetric and symmetric vibrations of the CH_3 group; a weak absorption band at 2928 cm^{-1}, which could be assigned to vibrations of the CH_2 group; and a strong absorption band of the C=O group at 1728 cm^{-1}, which is characteristic of the carboxylic acid ester group. The copolymerization of DAAM in the case of copolymers of Series 2 was evidenced

by the absorption band at 1535 cm^{-1}, which could be assigned to the N–H bond. All the copolymers of Series 2 also exhibited a weak absorption band at 1640 cm^{-1} corresponding to the N=C bond, which proved that the keto-hydrazide reaction took place in the coating films [74]. The copolymerization with TFEMA was manifested by absorption bands at 1280 and 650 cm^{-1}, which are characteristics of C–F stretching and C–F wagging, respectively.

Table 4. DLS results for the prepared latexes differing in the fluorination of the second-step polymer, emulsifier type, and covalent crosslinking strategy.

Sample	After the First Step		After the Completed Polymerization	
	Particle Diameter (nm)	Polydispersity Index (%)	Particle Diameter (nm)	Polydispersity Index (%)
Series 1: No crosslinking				
D_1	96.3 ± 0.6	5.3 ± 3.6	123.4 ± 0.8	3.4 ± 2.8
H_1	90.6 ± 0.4	4.2 ± 3.8	114.3 ± 0.9	5.3 ± 3.9
D_{1_F}	95.8 ± 1.0	3.8 ± 2.0	122.4 ± 0.7	2.6 ± 1.7
H_{1_F}	91.4 ± 0.8	4.4 ± 2.8	116.8 ± 1.2	4.6 ± 3.2
Series 2: Keto-hydrazide crosslinking				
D_2	97.1 ± 0.9	3.2 ± 2.6	120.4 ± 1.0	3.4 ± 2.3
H_2	87.8 ± 1.1	2.6 ± 1.4	112.3± 1.0	4.3 ± 2.8
D_{2_F}	103.1 ± 1.3	5.1 ± 4.0	128.6 ± 1.2	2.4 ± 1.6
H_{2_F}	96.3 ± 0.7	3.5 ± 1.9	120.2 ± 1.4	5.0 ± 3.2
Series 3: ALMA crosslinking				
D_3	96.8 ± 1.2	3.4 ± 3.1	123.7 ± 1.0	2.8 ± 1.9
H_3	89.9 ± 1.0	4.6 ± 4.0	114.7 ± 0.7	2.5 ± 1.4
D_{3_F}	98.2 ± 1.6	3.8 ± 2.4	124.8 ± 1.1	2.6 ± 1.7
H_{3_F}	92.4 ± 0.9	4.2 ± 2.7	118.4 ± 1.5	5.2 ± 4.0
Series 4: Keto-hydrazide and ALMA crosslinking				
D_4	95.1 ± 1.1	4.3 ± 3.1	118.3 ± 1.2	4.8 ± 4.6
H_4	82.0 ± 1.2	5.6 ± 4.4	105.7 ± 1.1	2.6 ± 1.8
D_{4_F}	97.5 ± 1.5	5.8 ± 4.0	121.1 ± 1.1	3.3 ± 2.5
H_{4_F}	80.9 ± 0.6	4.8 ± 3.7	102.5 ± 0.8	4.2 ± 3.2

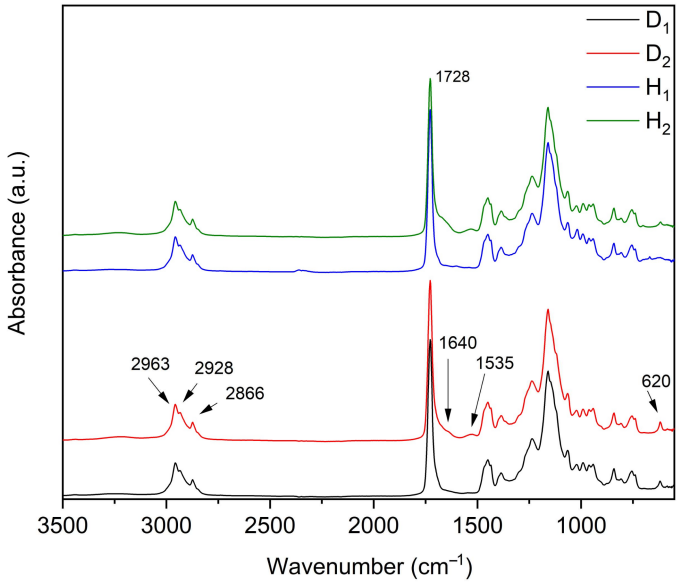

Figure 1. FT-IR absorption spectra of fluorine-free copolymer samples of Series 1 and 2.

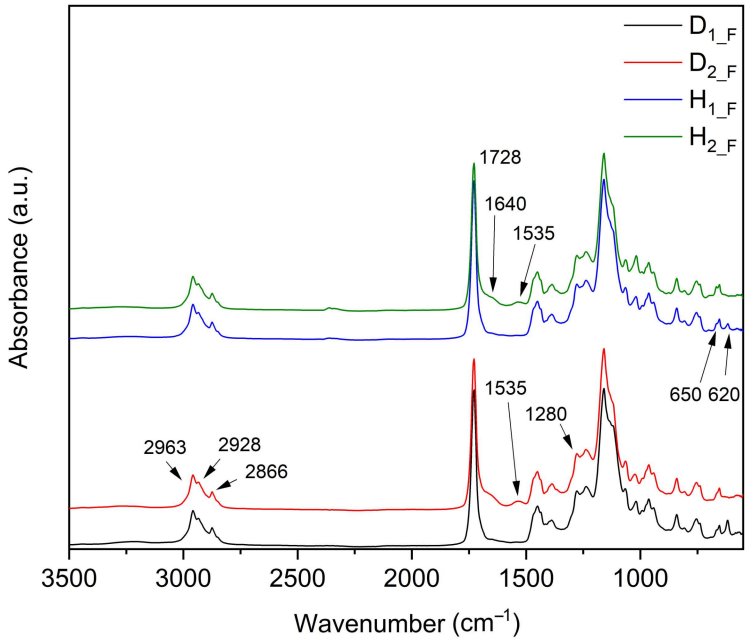

Figure 2. FT-IR absorption spectra of fluorinated copolymer samples of Series 1 and 2.

In addition, the chemical structures of copolymer films prepared from the polyacrylate latexes were studied in terms of the degree of crosslinking, which was presumed based on the results of M_c and crosslink density (see Table 5). As expected, the highest degree of crosslinking was achieved in the case of the films of Series 4, employing both interparticle and intraparticle covalent crosslinking (occurring between adjacent polymer particles and on the molecular level between the polymer chains, respectively). A dense polymer network was also found for the copolymers of Series 3, where intraparticle crosslinking was introduced due to ALMA copolymerization. However, a significant degree of crosslinking was even detected in the cases of copolymers H_1 and H_{1_F} of Series 1, where no crosslinking strategy was proposed. The networking in these copolymers could be ascribed to intermolecular chain transfer reactions to the polymer owing to BA copolymerization [75,76]. When comparing corresponding copolymers differing in emulsifier type, a higher degree of crosslinking was always determined in the case of the H-designed copolymers, which may indicate a higher molecular weight of the copolymers prepared using the polymerizable emulsifier [77] on the one hand, or to a higher quality of coalescence and polymer chain interdiffusion in the case of the polymerizable-emulsifier-based films on the other hand.

3.2. Water Resistance of Coating Films

The water resistance, hydrophobicity, and surface properties of latex coating films are usually closely related. We monitored the water resistance of the coating films according to water absorption (i.e., the amount of distilled water captured by a latex film) and water whitening. It has been documented in several scientific papers [2,31,77–81] that the water resistance of latex films is usually related significantly to their crosslink density, where the stiffness of the polymer network decreases the extent of water penetration and prevents the growth of water domains. In the case of the water whitening effect, it is supposed that only water domains exceeding a certain dimension can entail the effect of water whitening [82,83].

Table 5. Degree of crosslinking introduced into latex copolymers differing in the fluorination of the second-step polymer, emulsifier type, and covalent crosslinking strategy in terms of the average molar mass between crosslink junctions (M_c), and crosslink density.

Sample	M_c (g/mol)	Crosslink Density $\times$ 10^{-6} (moles/cm^3)
Series 1: No crosslinking		
D_1	NA [a]	NA [a]
H_1	240,600 ± 27,000	4.3 ± 0.6
D_{1_F}	NA [a]	NA [a]
H_{1_F}	148,200 ± 11,900	7.5 ± 0.6
Series 2: Keto-hydrazide crosslinking		
D_2	58,500 ± 700	18.8 ± 0.2
H_2	50,700 ± 2500	21.8 ± 1.1
D_{2_F}	44,600 ± 5300	24.9 ± 3.0
H_{2_F}	35,200 ± 3400	31.5 ± 3.1
Series 3: ALMA crosslinking		
D_3	18,100 ± 2500	61.7 ± 8.8
H_3	6800 ± 200	162.1 ± 5.1
D_{3_F}	12,900 ± 900	85.7 ± 6.2
H_{3_F}	6300 ± 300	175.0 ± 7.7
Series 4: Keto-hydrazide and ALMA crosslinking		
D_4	5600 ± 200	197.8 ± 4.3
H_4	3800 ± 100	289.3 ± 4.6
D_{4_F}	3400 ± 200	322.5 ± 17.4
H_{4_F}	2800 ± 50	392.2 ± 5.2

[a] Value could not be obtained because the gel polymer remained trapped in the extraction cartridge.

It was found that similar trends emerged in the case of both the water absorption and water whitening testing (see Figures 3 and 4). Concerning the crosslinking strategy, theoretical postulates (the higher the network density, the greater the decrease in the water sensitivity of coating films) were not fulfilled completely. The most densely crosslinked coating films of Series 4, engaging inter- and intraparticle covalent crosslinking, exhibited the lowest water sensitivity, but the moderately crosslinked films of Series 2 (using keto-hydrazide crosslinking chemistry) and the films of Series 3, (crosslinked by ALMA copolymerization) exhibited relatively high levels of water absorption and water whitening similar to (or in some cases even exceeding) the water sensitivity results of the noncrosslinked or slightly crosslinked films of Series 1. The reasons for this behavior may be (I) the sufficient elasticity of the moderately crosslinked polymer network and, concurrently, (II) a higher polarity introduced into the chemical structure due to the presence of keto-hydrazide chemistry in the case of Series 2; and (III) a poor coalescence quality of coating films of Series 3, which resulted in both increased water penetration and the growth of water domains. Focusing on emulsifier type, the coating films containing the polymerizable emulsifier always exhibited lower water sensitivity. This effect could be attributed to smaller interstices filled only with water-soluble salts originating from the persulfate initiator (in contrast to the general-emulsifier-based films comprising larger interstices also containing desorbed emulsifiers), resulting in a reduction in osmotic pressure and a suppression of water penetration. This phenomenon may also indicate a better coalescence quality (a higher level of chain interdiffusion) of the polymerizable-emulsifier-based latex coatings, probably because of more extensive hydration of the shell polymer due to the presence of a polymerized emulsifier. The phenomenon of the formation of a hydration shell, leading to plasticization by water molecules in the case of latex polymers [84], has been also observed in biological and nonbiological polymers [85–88]. Regarding the fluorination of the second-step polymer, it was found that the fluorinated coatings comprising the general emulsifier displayed slightly increased water resistance compared with the

corresponding fluorine-free coatings. However, this phenomenon was not confirmed in the case of polymerizable-emulsifier-based coatings. Hence, it can be concluded that the effect of perfluoroethyl groups in the polymer structure on the water sensitivity of the coating films was shown to be minor.

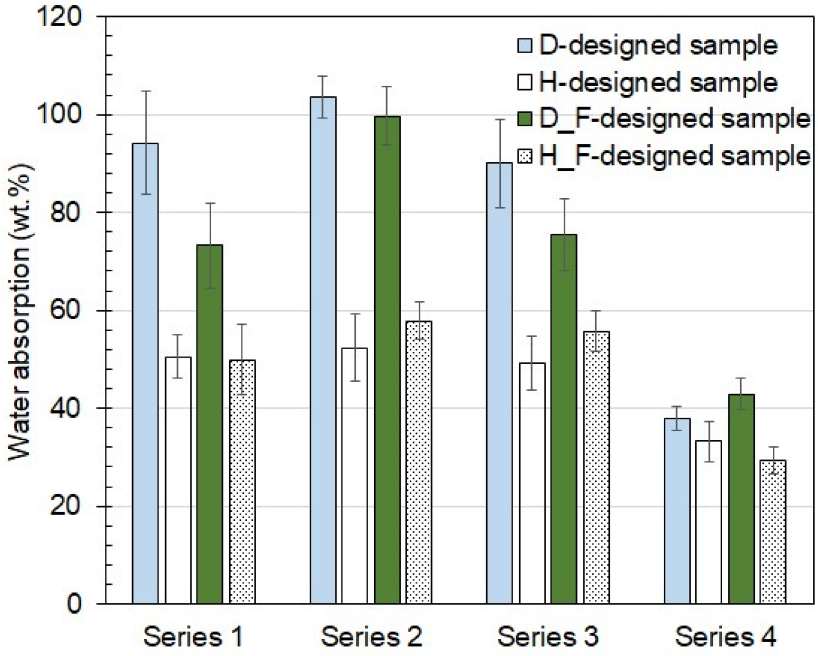

Figure 3. Water absorption of coating films (30-day-long water exposure).

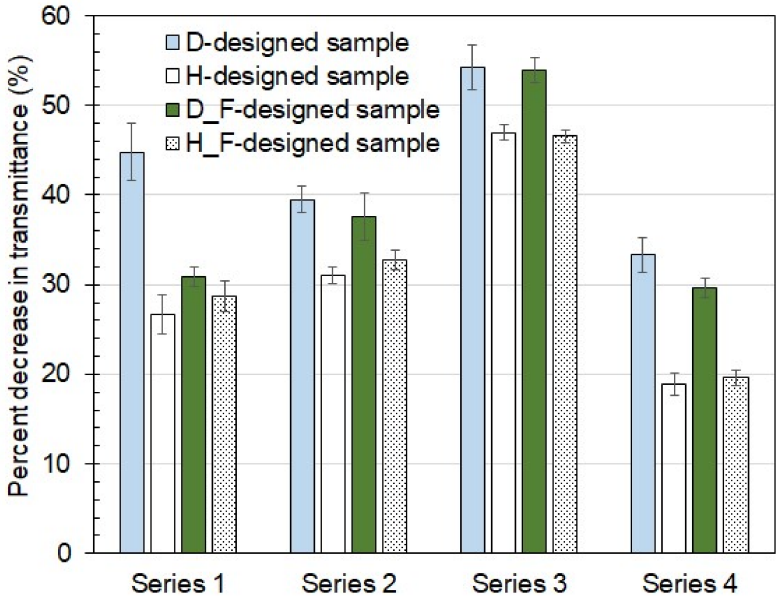

Figure 4. Water whitening of coating films expressed by a decrease in transmittance (1-day-long water exposure).

3.3. Surface Properties of Latex Films

The mutual effects of fluorinated monomer copolymerization, crosslinking strategy, and the use of a polymerizable emulsifier on the wettability of latex coatings were studied using WCA measurements. WCA is commonly used as a criterion for the evaluation of the level of hydrophobicity (hydrophilicity) of a solid surface. Nonpolar (hydrophobic) or polar (hydrophilic) groups, which are the constituent parts of polymer chains, can orientate to the interior of the coating film or towards the interface, depending on how the polarity

of the environment around the coating film changes, resulting in the variation in coating film wettability. Therefore, we tested the wettability of dried coating films before and after 1-day-long immersion in distilled water. The results of the WCA measurements are presented in Figure 5. It was confirmed that all the fluorinated coatings, regardless of the employed crosslinking strategy, had a hydrophobic character. The fluorinated latex coatings of Series 1 (D_{1_F} and H_{1_F}) even exhibited WCA values around 100°, which proved that the fluorinated compositions not employing a specific crosslinking strategy were the most favorable for achieving the highest possible coating hydrophobicity. This phenomenon could be related to the sufficient mobility of noncrosslinked (or slightly crosslinked) polymer chains, which facilitated the orientation of perfluoroethyl groups to the air-film interface during film drying. It was further shown that the type of the applied covalent crosslinking strategy did not affect the level of wettability of the coatings significantly. Nevertheless, it was proved that introducing crosslinking into latex films limited achieving a high level of coating hydrophobicity in the case of the fluorinated latex compositions, most likely due to the fixation of fluorine groups in the interior of latex particles. Focusing on the results of wettability in terms of the emulsifier type, the coating films with the polymerizable emulsifier always exhibited higher WCA values, which could be explained by smaller interstices (containing only initiator-based salts), resulting in lower surface polarity. Considering the effect of water exposure, no significant change in wettability was found for all the tested coatings except the fluorinated coating films of Series 1 (D_{1_F} and H_{1_F}). For these samples, the absence (or low level) of crosslinking allowed the perfluoroethyl groups to hide from the periphery to the inside of polymer particles when the coating films were in contact with water. After the immersion test, these coatings exhibited a similar level of wettability to the corresponding crosslinked coatings.

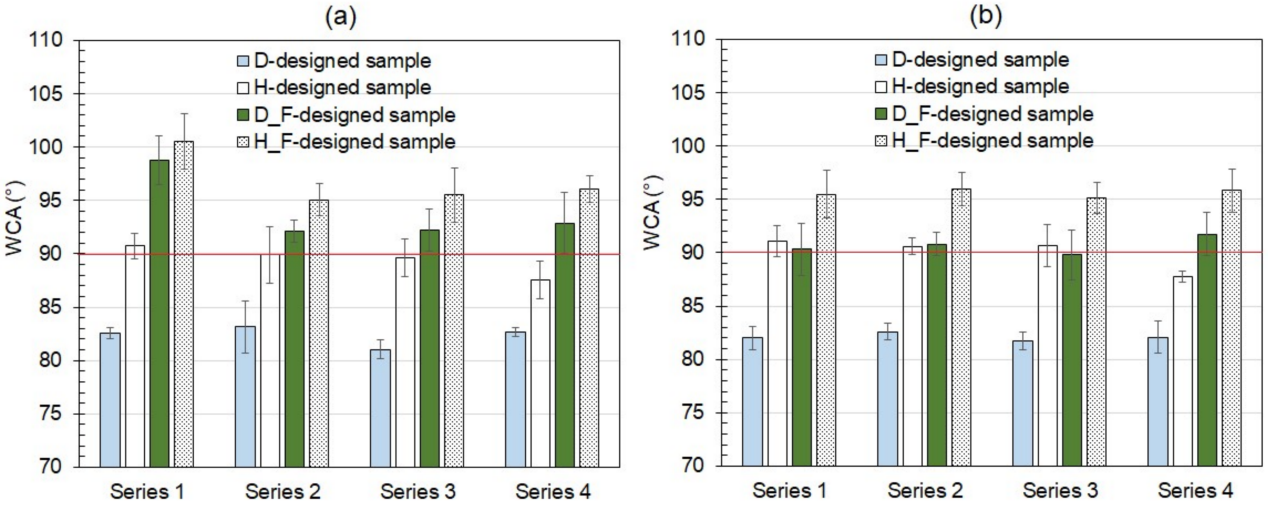

Figure 5. Wettability of coatings expressed in terms of water contact angle: (**a**) before exposure to distilled water; (**b**) after 1-day-long exposure to distilled water.

As optical microscopy did not reveal significant differences between the surface appearances of the individual coating samples at the macroscopic level (see Figure S1 in Supplementary Materials), the surface topography of the coatings was evaluated using AFM. The AFM analysis revealed fundamental differences between coating materials comprising the general and the polymerizable emulsifiers, whereas no significant difference in surface topography was found considering the level of crosslinking and fluorination of the second-step polymer. AFM images of the coating representatives D_4 and H_4, illustrating a distinction in the surface topography between the D-designed and the H-designed coatings, are shown in Figure 6 (almost identical results were also obtained for the D-designed and the H-designed coatings of other series, regardless of the fluorination, so these images are not shown). It was observed that the surfaces of the general-emulsifier-

based coatings (represented by the sample D_4) exhibited the relict of spherical particles having a lateral diameter of about 150 nm with a typical height difference below 10 nm, whereas the surfaces of the polymerizable-emulsifier-based coatings (illustrated by the example of the coating sample H_4) were found to be almost without the relict of original latex spheres, indicating a better coalescence ability, which was also visible in different values of residual roughness in the form of the root mean square [80] of 0.2 and 2.3 nm for H_4 and D_4, respectively. The reason for the smooth surface of the H-designed coatings may lie in the covalent bonding of emulsifier molecules polymer chains, disabling their desorption, migration, and formation of chemically different interstices between latex particles, which probably resulted in better coalescence (chain interpenetration).

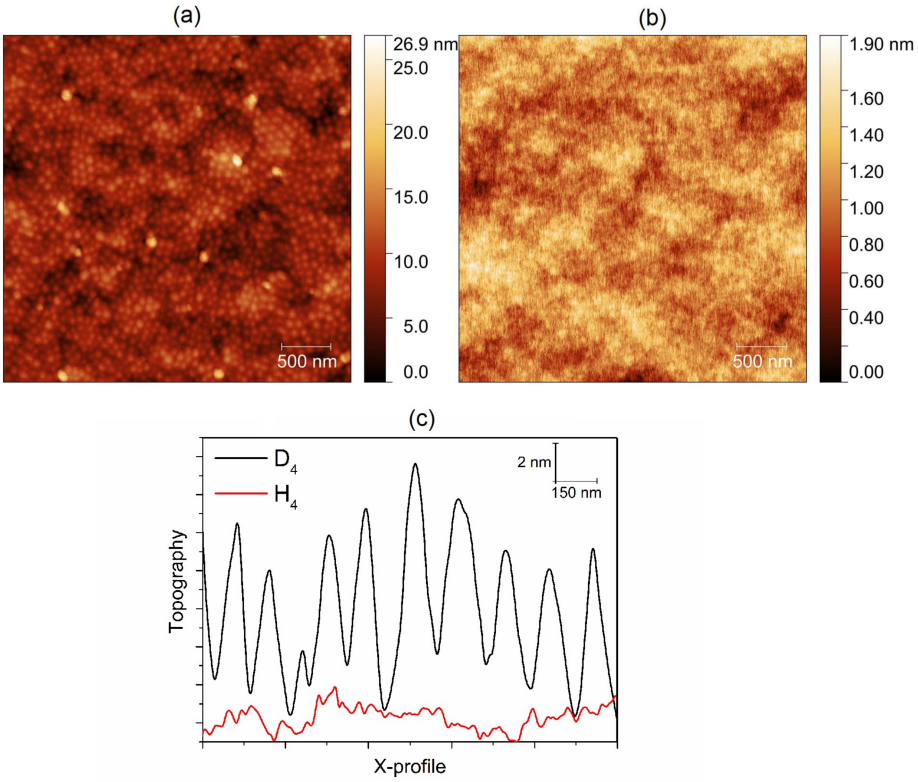

Figure 6. AFM images of latex coating films performed in the topographical mode: (**a**) sample D_4; (**b**) sample H_4; (**c**) topographical profiles for samples D_4 and H_4.

Latex coatings, like any other coating materials, are at the risk of developing microcracks during their service life due to external mechanical forces, which can lead to the subsequent exposure of a protected substrate to oxygen and atmospheric moisture. Therefore, the self-healing behavior of latex coatings, providing full or partial recovery of the protective coating film, has been extensively explored to provide longer durability and to meet the application requirements of different occasions [89–92]. In this study, the self-healing effect of coatings in terms of their recovery dynamics [93] was evaluated according to the kinetics of the topography changes of a scratch induced by a surgical needle into a latex film. The topography was observed with a digital holography microscope on an identical line for different time intervals of recovery. The depth of the scratch was the basic parameter, and the relative recovery was normalized for an initial scratch depth of ca. 1200 nm at 0 min. Similarly, different recovery dynamics of the coatings were observed concerning the type of emulsifier used, whereas no evident effects of crosslinking strategy and polymer fluorination were proved (see Figure 7 illustrating the recovery effect for the samples D_4 and H_4, representing the general-emulsifier-based and the polymerizable-emulsifier-based coatings, respectively). It was demonstrated that no significant topography changes of the scratch occurred within 60 min of the measurement in the

case of all the general-emulsifier-based coatings (see Figure 7a showing representative D_4), whereas the depth of the scratch decreased significantly in the case of all the coatings based on the polymerizable emulsifier (see Figure 7b illustrating a typical self-healing effect of the H-designed coatings with the example of sample H_4, where the scratch depth dropped from an initial value of 1200 nm to half of the initial value (recovery half-time) within 14 min and further decreased to about 200 nm within 60 min). It was also demonstrated for the H-designed coatings that the kinetics of relative recovery fulfilled the exponential decay (see Figure 7c), and the residual scratch depth was calculated as about 15%, related to the initial scratch depth at the steady-state conditions. To the best of our knowledge, the self-healing performance of latex materials synthesized using polymerizable emulsifiers occurring without external input in the manner of a memory effect has not been described in the relevant literature. We assume that the recovery process could be attributed to an increased level of polymer chain interpenetration, which probably allowed the inherent reversibility of noncovalent intermolecular bonding in the well-coalesced film. Nevertheless, the explanation of this phenomenon, indicating a certain level of thermoplasticity of the latex polymer film, deserves a more detailed and sophisticated study, which is not the subject of this work but may be considered for future studies.

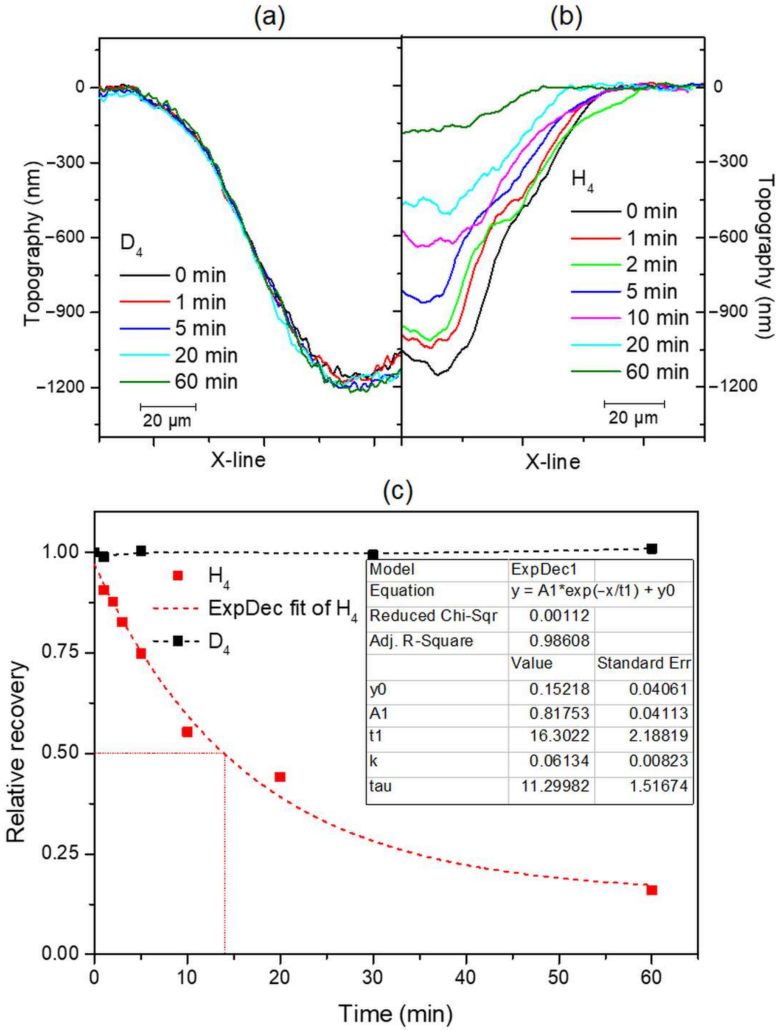

Figure 7. Illustration of the surface self-healing (recovery) effect based on the topography of scratches: (**a**) sample D_4; (**b**) sample H_4; (**c**) the kinetics of relative recovery for samples D_4 and H_4. The experimental values of recovery kinetics were fitted by the exponential decay function. The measurements were performed at RT and 30 ± 1% RH.

4. Conclusions

In this paper, the effects of the fluorination of latex acrylic polymers, emulsifier type, and crosslinking strategy on the water resistance, hydrophobicity, and surface properties of coating films were investigated. As expected, the most densely crosslinked coating films engaging intra- and interparticle covalent crosslinking (provided by ALMA copolymerization and keto-hydrazide chemistry, respectively) provided the highest water resistance from the point of view of low water absorption and water whitening, whereas the moderately crosslinked films employing keto-hydrazide crosslinking or ALMA copolymerization, exhibited relatively high levels of water absorption and water whitening similar to the latex films designed without any crosslinking strategy. This effect was attributed to the sufficient elasticity of the moderately crosslinked polymer network, which allowed increased water penetration and the growth of water domains. It was also shown that the coating films made of the polymerizable-emulsifier-based latexes provided higher water resistance. This phenomenon was explained by better coalescence quality and the existence of smaller polar interstices in the case of the polymerizable-emulsifier-based latex films. The fluorination of latex polymer was shown to increase the water resistance of coating films only minimally, but it was proved to provide the hydrophobic character of coatings. Fluorinated compositions without covalent crosslinking were found to be the most favorable for achieving the highest possible hydrophobicity of coatings. In this case, the mobility of noncrosslinked polymer chains facilitated the orientation of fluorine groups to the air-film interface during film drying. Further, fundamental differences between the surface topography of coatings comprising the general and the polymerizable emulsifiers were found, revealing the better coalescence quality and the self-healing effect of the polymerizable emulsifier-based coating materials. It can be summarized that highly water-resistant and hydrophobic polyacrylate "smart" latex coatings, being able to recover their structural integrity without external input, were prepared in the case of simultaneously (I) using a polymerizable anionic emulsifier (HITENOL AR-10) in the process of emulsion polymerization; (II) introducing intra- and interparticle covalent crosslinking by ALMA copolymerization and keto-hydrazide self-crosslinking chemistry, respectively; and (III) copolymerizing TFEMA into the second-step polymer.

Supplementary Materials: The following supporting information can be downloaded at: https://www.mdpi.com/article/10.3390/coatings12081150/s1, Figure S1: Macro surface appearance of latex coating films: (a) Sample D_0; (b) Sample H_0.

Author Contributions: Conceptualization, J.M.; methodology, J.M., E.C. and P.K.; investigation, P.K., E.C., R.S., L.Z., A.K. and M.K.; resources, J.M.; data curation, J.M., P.K. and L.Z.; writing—original draft preparation, J.M.; writing—review and editing, J.M.; visualization, J.M.; supervision, J.M. All authors have read and agreed to the published version of the manuscript.

Funding: This research received no external funding.

Institutional Review Board Statement: Not applicable.

Informed Consent Statement: Not applicable.

Data Availability Statement: Not applicable.

Conflicts of Interest: The authors declare no conflict of interest.

References

1. Rodríguez, R.; Alarcón, C.; Ekanayake, P.; McDonald, P.J.; Keddie, J.L.; Barandiaran, M.J.; Asua, J.M. Correlation of silicone incorporation into hybrid acrylic coatings with the resulting hydrophobic and thermal properties. *Macromolecules* **2008**, *41*, 8537–8546. [CrossRef]
2. Machotová, J.; Černošková, E.; Honzíček, J.; Šňupárek, J. Water sensitivity of fluorine-containing polyacrylate latex coatings: Effects of crosslinking and ambient drying conditions. *Prog. Org. Coat.* **2018**, *120*, 266–273. [CrossRef]
3. Bassett, D.R. Hydrophobic coatings from emulsion polymers. *J. Coat. Technol.* **2001**, *73*, 43–55. [CrossRef]
4. Xie, Y.; Wang, R.; Li, S.; Xiang, T.; Zhao, C.-S. A robust way to prepare blood-compatible and anti-fouling polyethersulfone membrane. *Colloids Surf. B Biointerfaces* **2016**, *146*, 326–333. [CrossRef] [PubMed]

5. Oldani, V.; del Negro, R.; Bianchi, C.L.; Suriano, R.; Turri, S.; Pirola, C.; Sacchi, B. Surface properties and anti-fouling assessment of coatings obtained from perfluoropolyethers and ceramic oxides nanopowders deposited on stainless steel. *J. Fluorine Chem.* **2015**, *180*, 7–14. [CrossRef]
6. Zheng, S.X.; Li, J.H. Inorganic-organic sol gel hybrid coatings for corrosion protection of metals. *J. Sol.-Gel Sci. Technol.* **2010**, *54*, 174–187. [CrossRef]
7. Chiong, S.J.; Goh, P.S.; Ismail, A.F. Novel hydrophobic PVDF/APTES-GO nanocomposite for natural gas pipelines coating. *J. Nat. Gas Sci. Eng.* **2017**, *42*, 190–202. [CrossRef]
8. Zhou, C.L.; Lu, X.; Xin, Z.; Liu, J.; Zhang, Y.F. Hydrophobic benzoxazine-cured epoxy coatings for corrosion protection. *Prog. Org. Coat.* **2013**, *76*, 1178–1183. [CrossRef]
9. Kapridaki, C.; Maravelaki-Kalaitzaki, P. TiO_2-SiO_2-PDMS nano-composite hydrophobic coating with self-cleaning properties for marble protection. *Prog. Org. Coat.* **2013**, *76*, 400–410. [CrossRef]
10. Li, X.M.; Reinhoudt, D.; Crego-Calama, M. What do we need for a superhydrophobic surface? A review on the recent progress in the preparation of superhydrophobic surfaces. *Chem. Soc. Rev.* **2007**, *36*, 1350–1368. [CrossRef]
11. Il'darkhanova, F.I.; Mironova, G.A.; Bogoslovsky, K.G.; Men'shikov, V.V.; Bykov, E.D. Development of paint coatings with superhydrophobic properties. *Prot. Met. Phys. Chem. Surf.* **2012**, *48*, 796–802. [CrossRef]
12. López, A.B.; de la Cal, J.C.; Asua, J.M. Highly hydrophobic coatings from waterborne latexes. *Langmuir* **2016**, *32*, 7459–7466. [CrossRef]
13. Chen, L.; Shao, T.; Gong, Y.; Wang, X.; Sun, Z. Synthesis and properties of cross-linked fluorine and silicon VAc-VeoVa polymer latex emulsified by green mixed surfactant. *J. Polym. Mater.* **2018**, *35*, 281–293. [CrossRef]
14. Xu, W.; An, Q.; Hao, L.; Zhang, D.; Zhang, M. Synthesis and characterization of self-crosslinking fluorinated polyacrylate soap-free latices with core-shell structure. *App. Surf. Sci.* **2013**, *268*, 373–380. [CrossRef]
15. Wang, X.; Bao, Z.; Chen, L. Preparation of cross-linked and fluorine-silicon modified acrylate emulsion by using mixed green surfactants. *J. Polym. Mater.* **2016**, *33*, 685–696.
16. Shayegan, Z.; Lee, C.S.; Haghighat, F. Effect of surface fluorination of P25-TiO_2 coated on nickel substrate for photocatalytic oxidation of methyl ethyl ketone in indoor environments. *J. Environ. Chem. Eng.* **2019**, *7*, 103390. [CrossRef]
17. Zhang, N.; Li, D.; Mu, M.; Lu, M. Partially fluorinated UiO-66-NH_2 (Zr): Positive effect of the fluorine moiety on the adsorption capacity for environmental pollutants of metal-organic frameworks. *Chem. Eng. J.* **2022**, *448*, 137467. [CrossRef]
18. Cui, X.; Zhong, S.; Gao, Y.; Wang, H. Preparation and characterization of emulsifier-free core-shell interpenetrating polymer network-fluorinated polyacrylate latex particles. *Colloids Surf. A Physicochem. Eng. Asp.* **2008**, *324*, 14–21. [CrossRef]
19. Cui, X.; Zhong, S.; Wang, H. Emulsifier-free core-shell polyacrylate latex nanoparticles containing fluorine and silicon in shell. *Polymer* **2007**, *48*, 7241–7248. [CrossRef]
20. Anton, D. Surface-fluorinated coatings. *Adv. Mater.* **1998**, *10*, 1197–1205. [CrossRef]
21. Thomas, R.R.; Anton, D.R.; Graham, W.F.; Darmon, M.J.; Stika, K.M. Films containing reactive mixtures of perfluoroalkylethyl methacrylate copolymers and fluorinated isocyanates: Synthesis and surface properties. *Macromolecules* **1998**, *31*, 4595–4604. [CrossRef]
22. Zhang, C.; Chen, Y. Investigation of fluorinated polyacrylate latex with core-shell structure. *Polym. Int.* **2005**, *54*, 1027–1033. [CrossRef]
23. Morita, M.; Ogisu, H.; Kubo, M. Surface properties of perfluoroalkylethyl acrylate/n-alkyl acrylate copolymers. *J. Appl. Polym. Sci.* **1999**, *73*, 1741–1749. [CrossRef]
24. Schmidt, D.L.; Brady, R.F.; Lam, K.J.; Schmidt, D.C.; Chaudhury, M.K. Contact angle hysteresis, adhesion, and marine biofouling. *Langmuir* **2004**, *20*, 2830–2836. [CrossRef] [PubMed]
25. Lü, T.; Qi, D.; Zhang, D.; Liu, Q.; Zhao, H. Fabrication of self-cross-linking fluorinated polyacrylate latex particles with core-shell structure and film properties. *React. Funct. Polym.* **2016**, *104*, 9–14. [CrossRef]
26. Chen, Y.; Zhang, C.; Wang, Y.; Cheng, S.; Chen, P. Study of self-crosslinking acrylate latex containing fluorine. *J. Appl. Polym. Sci.* **2003**, *90*, 3609–3616. [CrossRef]
27. Chen, L.; Bao, Z.; Fu, Z.; Li, W. Preparation and characterisation of novel cross-linked poly (IBOMA-BA-DFMA) latex. *Pigment. Resin Technol.* **2015**, *44*, 333–338. [CrossRef]
28. Chen, L.; Wu, F. Preparation and characterization of novel self cross-linking fluorinated acrylic latex. *J. Appl. Polym. Sci.* **2012**, *123*, 1997–2002. [CrossRef]
29. Xiao, X.Y.; Xu, R. Preparation and surface properties of core-shell polyacrylate latex containing fluorine and silicon in the shell. *J. Appl. Polym. Sci.* **2011**, *119*, 1576–1585. [CrossRef]
30. Liu, Z.; Zhao, Y.H.; Zhou, J.W.; Yuan, X.Y. Synthesis and characterization of core-shell polyacrylate latex containing fluorine/silicone in the shell and the selfstratification film. *Colloid Polym. Sci.* **2012**, *290*, 203–211. [CrossRef]
31. Ruckerova, A.; Machotova, J.; Svoboda, R.; Pukova, K.; Bohacik, P.; Valka, R. Ambient temperature self-crosslinking latices using low generation PAMAM dendrimers as inter-particle crosslinking agents. *Prog. Org. Coat.* **2019**, *119*, 91–98. [CrossRef]
32. Tillet, G.; Boutevin, B.; Ameduri, B. Chemical reactions of polymer crosslinking and post-crosslinking at room temperature. *Prog. Polym. Sci.* **2011**, *36*, 191–217. [CrossRef]
33. Gonzáles, I.; Asua, J.M.; Leiza, J.R. Crosslinking in acetoacetoxy functional waterborne crosslinkable latexes. *Macromol. Symp.* **2006**, *243*, 53–62. [CrossRef]

34. Nakayama, Y. Development of novel aqueous coatings which meet the requirements of ecology-conscious society: Novel cross-linking system based on the carbonyl-hydrazide reaction and its applications. *Prog. Org. Coat.* **2004**, *51*, 280–299. [CrossRef]
35. Koukiotis, C.G.; Karabela, M.M.; Sideridou, I.D. Mechanical properties of films of latexes based on copolymers BA/MMA/DAAM and BA/MMA/VEOVA-10/DAAM and the corresponding self-crosslinked copolymers using the adipic acid dihydrazide as crosslinking agent. *Prog. Org. Coat.* **2012**, *75*, 106–115. [CrossRef]
36. Koukiotis, C.; Sideridou, I.D. Synthesis and characterization of latexes based on copolymers BA/MMA/DAAM and BA/MMA/VEOVA-10/DAAM and the corresponding 1K crosslinkable binder using the adipic acid dihydrazide as crosslinking agent. *Prog. Org. Coat.* **2010**, *69*, 504–509. [CrossRef]
37. Zhang, X.; Liu, Y.; Huang, H.; Li, Y.; Chen, H. The diacetone acrylamide crosslinking reaction and its control of core-shell polyacrylate lattices at ambient temperature. *J. Appl. Polym. Sci.* **2012**, *123*, 1822–1832. [CrossRef]
38. Li, H.; Kan, C.; Du, Y.; Liu, D. Effects of the amount of diacetone acrylamide on the properties of styrene-acrylic copolymer latexes and their films. *Polym. Prep.* **2002**, *43*, 413–414.
39. Kessel, N.; Illsley, D.R.; Keddie, J.L. The diacetone acrylamide crosslinking reaction and its influence on the film formation of an acrylic latex. *J. Coat. Technol. Res.* **2008**, *5*, 285–297. [CrossRef]
40. Kang, K.; Kan, C.Y.; Du, Y.; Liu, D.S. Synthesis and properties of soap-free poly(methyl methacrylate-ethyl acrylate-methacrylic acid) latex particles prepared by seeded emulsion polymerization. *Eur. Polym. J.* **2005**, *41*, 439–445. [CrossRef]
41. Xu, G.; Deng, L.; Wen, X.; Pi, P.; Zheng, D.; Cheng, J.; Yang, Z. Synthesis and characterization of fluorine-containing poly-styrene-acrylate latex with core-shell structure using a reactive surfactant. *J. Coat. Technol. Res.* **2011**, *8*, 401–407. [CrossRef]
42. Aramendia, E.; Barandiaran, M.J.; Grade, J.; Blease, T.; Asua, J.M. Polymerization of high-solids-content acrylic latexes using a nonionic polymerizable surfactant. *J. Polym. Sci. A Polym. Chem.* **2002**, *40*, 1552–1559. [CrossRef]
43. Yang, S.F.; Xiong, P.T.; Gong, T.; Lu, D.P.; Guan, R. St-BA copolymer emulsion prepared by using novel cationic maleic dialkyl polymerizable emulsifier. *Eur. Polym. J.* **2005**, *41*, 2973–2979. [CrossRef]
44. Filet, A.; Guillot, J.; Hamaide, T.; Guyot, A. Emulsion copolymerization of styrene with a nonionic styrenic polymerizable surfactant. *Polym. Advan. Technol.* **1995**, *6*, 465–472. [CrossRef]
45. Chern, C.S.; Chen, Y.C. Semibatch emulsion polymerization of butyl acrylate stabilized by a polymerizable surfactant. *Polym. J.* **1996**, *28*, 627–632. [CrossRef]
46. Schoonbrood, H.A.S.; Asua, J.M. Reactive surfactants in heterophase polymerization. 9. Optimum surfmer behaviour in emulsion polymerization. *Macromolecules* **1997**, *30*, 6034–6041. [CrossRef]
47. Guyot, A. Advances in reactive surfactants. *Adv. Colloid Interface Sci.* **2004**, *108–109*, 3–22. [CrossRef]
48. Hellgren, A.C.; Weissenborn, P.; Holmberg, K. Surfactants in water-borne paints. *Prog. Org. Coat.* **1999**, *35*, 79–87. [CrossRef]
49. Chern, C.S.; Chen, Y.C. Stability of the polymerizable surfactant stabilized latex particles during semibatch emulsion polymerization. *Colloid Polym. Sci.* **1997**, *275*, 124–130. [CrossRef]
50. Xiao, X.; Wang, Y. Emulsion polymerization of fluorinated acrylate in the presence of a polymerizable emulsifier. *Colloids Surf. A: Physicochem. Eng. Asp.* **2009**, *348*, 151–156. [CrossRef]
51. Wu, Z.; Zhong, C.Z.; Song, Y.; Zhang, Y.Q. Preparation and characterization of novel acrylate emulsiones with ketone-hydrazide crosslinking structure based on application of reactive emulsifier. *Adv. Mat. Res.* **2013**, *833*, 335–338. [CrossRef]
52. Hao, L.; An, Q.; Xu, W.; Zhang, D.; Zhang, M. Effect of polymerizable emulsifier and fluorine monomer on properties of self-crosslinking fluorinated polyacrylate soap-free latexes. *J. Polym. Res.* **2013**, *20*, 174. [CrossRef]
53. Ugelstad, J.; El-Aasser, M.S.; Vanderhoff, J.W. Emulsion polymerization: Initiation of polymerization in monomer droplets. *J. Polym. Sci. Polym. Lett. Ed.* **1973**, *11*, 503–513. [CrossRef]
54. Cheng, X.; Chen, Z.; Shi, T.; Wang, H. Synthesis and characterization of core-shell LIPN-fluorine-containing polyacrylate latex. *Colloids Surf. A Physicochem. Eng. Asp.* **2007**, *292*, 119–124. [CrossRef]
55. Ha, J.K.; Park, I.J. Preparation and characterization of core-shell particles containing perfluoroalkyl acrylate in the shell. *Macromolecules* **2002**, *35*, 6811–6818. [CrossRef]
56. Xu, W.; An, Q.F.; Hao, L.F.; Huang, L.X. Synthesis, film morphology and performance of cationic fluorinated polyacrylate emulsion with core-shell structure. *J. Appl. Polym. Sci.* **2012**, *125*, 2376–2383. [CrossRef]
57. Cheng, S.; Chen, Y.; Chen, Z. Core-shell latex containing fluorine polymer rich in shell. *J. Appl. Polym. Sci.* **2002**, *85*, 1147–1153. [CrossRef]
58. Jong, W.; In, J.P.; Kim, D.K. Surface properties of cote-shell particles containing perfluoroalkyl acrylate in shell. *Surf. Sci.* **2003**, *328*, 532–535.
59. Gao, J.; Wang, X. Synthesis and characterization of novel fluorine-containing polymer emulsion with core/shell structure. *J. Fluor. Chem.* **2006**, *127*, 282–286. [CrossRef]
60. Fox, T.G.; Flory, P.J. 2nd-Order transition temperatures and related properties of polystyrene. 1. Influence of molecular weight. *J. Appl. Phys.* **1950**, *21*, 581–591. [CrossRef]
61. Al Islam, M.A.; Rahman, A.F.M.M.; Iftekhar, S.; Salem, K.S.; Sultana, N.; Bari, M.L. Morphology, thermal stability, electrical, and mechanical properties of graphene incorporated poly (vinyl alcohol)-gelatin nanocomposites. *Int. J. Compos. Mater.* **2016**, *6*, 172–182.

62. Salem, K.S.; Lubna, M.M.; Rahman, A.M.; NurNabi, M.; Islam, R.; Khan, M.A. The effect of multiwall carbon nanotube additions on the thermo-mechanical, electrical, and morphological properties of gelatin-polyvinyl alcohol blend nanocomposite. *J. Compos. Mater.* **2015**, *49*, 1379–1391. [CrossRef]
63. Sperling, L.H. *Introduction to Physical Polymer Science*, 4th ed.; John Wiley & Sons: Hoboken, NJ, USA, 2005; pp. 427–473.
64. Flory, P.J.; Rehner, J. Statistical mechanics of cross-linked polymer networks II. Swelling. *J. Chem. Phys.* **1943**, *11*, 521–526. [CrossRef]
65. Tobing, S.; Klein, A. Molecular parameters and their relation to the adhesive performance of acrylic pressure-sensitive adhesives. *J. Appl. Polym. Sci.* **2001**, *79*, 2230–2244. [CrossRef]
66. Vandenburg, H.J.; Clifford, A.A.; Bartle, K.D.; Carlson, R.E.; Caroll, J.; Newton, I.D. A simple solvent selection method accelerated solvent extraction of additives from polymers. *Analyst* **1999**, *124*, 1707–1710. [CrossRef]
67. Knotek, P.; Chanova, E.; Rypacek, F. AFM Imaging and analysis of local mechanical properties for detection of surface pattern of functional groups. *Mat. Sci. Eng. C* **2013**, *33*, 1963–1968. [CrossRef]
68. Todorov, R.; Lozanova, V.; Knotek, P.; Černošková, E.; Vlček, M. Microstructure and ellipsometric modelling of the optical properties of very thin silver films for application in plasmonics. *Thin Solid Films* **2017**, *628*, 22–30. [CrossRef]
69. Knotek, P.; Tichý, L. Atomic force microscopy and atomic force acoustic microscopy characterization of photo-induced changes in some Ge-As-S amorphous films. *Thin Solid Films* **2009**, *517*, 1837–1840. [CrossRef]
70. Knotek, P.; Arsova, D.; Vateva, E.; Tichy, L. Photo-expansion in Ge-As-S amorphous film monitored by digital holographic microscopy and atomic force microscopy. *J. Optoelectron. Adv. Mater.* **2009**, *11*, 391–394.
71. Aguirreurreta, Z.; Cal, J.C.; Leiza, J.R. Anionic polymerizable surfactants and stabilizers in emulsion polymerization: A comparative study. *Macromol. React. Eng.* **2017**, *11*, 1600033. [CrossRef]
72. Mekki, S.; Saïdi-Besbes, S.; Elaïssari, A.; Valour, J.P.; Derdour, A. Novel polymerizable surfactants: Synthesis and application in the emulsion polymerization of styrene. *Polym. J.* **2010**, *42*, 401–405. [CrossRef]
73. Urquiola, M.B.; Dimonie, V.L.; Sudol, E.D.; El-Aasser, M.S. Emulsion polymerization of vinyl acetate using a polymerizable surfactant. I. Kinetic studies. *J. Appl. Polym. Sci. A Polym. Chem.* **1992**, *30*, 2619–2629. [CrossRef]
74. Pi, P.; Wang, W.; Wen, X.; Xu, S.; Cheng, J. Synthesis and characterization of low-temperature self-crosslinkable acrylic emulsion for PE film ink. *Prog. Org. Coat.* **2015**, *81*, 66–71. [CrossRef]
75. Podzimek, S.; Machotova, J.; Snuparek, J.; Vecera, M.; Prokupek, L. Characterization of molecular structure of acrylic copolymers prepared via emulsion polymerization using A4F-MALS technique. *J. Appl. Polym. Sci.* **2014**, *131*, 11178–11185. [CrossRef]
76. Plessis, C.; Arzamendi, G.; Leiza, J.R.; Alberdi, J.M.; Schoonbrood, H.A.; Charmot, D.; Asua, J.M. Seeded semibatch emulsion polymerization of butyl acrylate: Effect of the chain-transfer agent on the kinetics and structural properties. *J. Polym. Sci. A Polym. Chem.* **2001**, *39*, 1106–1119. [CrossRef]
77. Machotová, J.; Kalendová, A.; Steinerová, D.; Mácová, P.; Šlang, S.; Šňupárek, J.; Vajdák, J. Water-resistant latex coatings: Tuning of properties by polymerizable surfactant, covalent crosslinking and nanostructured ZnO additive. *Coatings* **2021**, *11*, 347. [CrossRef]
78. Winnik, M.A. Interdiffusion and crosslinking in thermoset latex films. *J. Coat. Technol.* **2002**, *74*, 49–63. [CrossRef]
79. Taylor, J.W.; Winnik, M.A. Functional latex and thermoset latex films. *JCT Res.* **2004**, *1*, 163–190. [CrossRef]
80. Tian, Y.; Du, E.; Abdelmola, F.; Qiang, Y.; Carlsson, L. A Rapid characterization of water diffusion in polymer specimens using a droplet-based method. *Langmuir* **2020**, *36*, 7309–7314. [CrossRef]
81. Machotová, J.; Kalendová, A.; Zlámaná, B.; Šňupárek, J.; Palarčík, J.; Svoboda, R. Waterborne coating binders based on self-crosslinking acrylic latex with embedded inorganic nanoparticles: A comparison of nanostructured ZnO and MgO as crosslink density enhancing agents. *Coatings* **2020**, *10*, 339. [CrossRef]
82. Jiang, B.; Tsavalas, J.G.; Sundberg, D.C. Water whitening of polymer films: Mechanistic studies and comparison between water and solvent borne films. *Prog. Org. Coat.* **2017**, *105*, 56–66. [CrossRef]
83. Liu, Y.; Gajawicz, A.M.; Rodin, V.; Soer, W.; Scheerder, J.; Satgurunathan, G.; McDonald, P.J.; Keddie, J.L. Explanations for water whitening in secondary dispersion and emulsion polymer films. *J. Polym. Sci. B Polym. Phys.* **2016**, *54*, 1658–1674. [CrossRef]
84. Tsavalas, J.G.; Sundberg, D.C. Hydroplasticization of polymers: Model predictions and application to emulsion polymers. *Langmuir* **2010**, *26*, 6960–6966. [CrossRef]
85. Cerveny, S.; Swenson, J. Water dynamics in the hydration shells of biological and non-biological polymers. *J. Chem. Phys.* **2019**, *150*, 234904. [CrossRef]
86. Salem, K.S.; Starkey, H.R.; Pal, L.; Lucia, L.; Jameel, H. The topochemistry of cellulose nanofibrils as a function of mechanical generation energy. *ACS Sustain. Chem. Eng.* **2019**, *8*, 1471–1478. [CrossRef]
87. Salem, K.S.; Naithani, V.; Jameel, H.; Lucia, L.; Pal, L. A systematic examination of the dynamics of water-cellulose interactions on capillary force-induced fiber collapse. *Carbohydr. Polym.* **2022**, *295*, 119856. [CrossRef]
88. Li, X.; Li, J.; Eleftheriou, M.; Zhou, R. Hydration and dewetting near fluorinated superhydrophobic plates. *J. Am. Chem. Soc.* **2006**, *128*, 12439–12447. [CrossRef]
89. Sopha, H.; Tesar, K.; Knotek, P.; Jäger, A.; Hromadko, L.; Macak, J.M. TiO_2 nanotubes grown on Ti substrates with different microstructure. *Mater. Res. Bull.* **2018**, *103*, 197–204. [CrossRef]
90. Mirabedini, S.M.; Dutil, I.; Gauquelin, L.; Yan, N.; Farnood, R.R. Preparation of self-healing acrylic latex coatings using novel oil-filled ethyl cellulose microcapsules. *Prog. Org. Coat.* **2015**, *85*, 168–177. [CrossRef]

91. Ataei, S.; Khorasani, S.N.; Neisiany, R.E. Biofriendly vegetable oil healing agents used for developing self-healing coatings: A review. *Prog. Org. Coat.* **2019**, *129*, 77–95. [CrossRef]
92. Cui, X.; Zhang, C.; Camilo, R.P.; Zhang, H.; Cobaj, A.; Soucek, M.D.; Zacharia, N.S. Self-healing latex containing polyelectrolyte multilayers. *Macromol. Mater. Eng.* **2018**, *303*, 1700596. [CrossRef]
93. Chen, Q.; Tian, M.; de Vos, K.; Kastelijn, M.; Peters, R.A.H.; Loos, J.; Scheerder, J. Recovery dynamics of acrylic coating surfaces under elevated relative humidity monitored by atomic force microscopy. *Prog. Org. Coat.* **2020**, *146*, 105712. [CrossRef]